Materials Today Sustainability 6 (2019) 100023

Contents lists available at ScienceDirect

Materials Today Sustainability

journal homepage: https://www.journals.elsevier.com/materials-today-sustainability

Amplified CO_2 reduction of greenhouse gas emissions with C2CNT carbon nanotube composites

S. Licht*, X. Liu, G. Licht, X. Wang, A. Swesi, Y. Chan

Dept. of Chemistry, George Washington University, Washington DC 20052, USA

ARTICLE INFO

Article history:
Received 27 March 2019
Received in revised form
3 July 2019
Accepted 13 August 2019
Available online 26 August 2019

Keywords:
Carbon nanotubes
Cement
Carbon mitigation
Cement composite
Carbon dioxide electrolysis
Carbon avoidance

ABSTRACT

Production of cement, aluminum, magnesium, titanium, and steel structural materials generate more than 2 gigatonnes of CO_2 globally per year. Replacement of structural materials with lightweight, stronger carbon nanotube (CNT) composites reduces the structural material's production aggregate requirements by achieving the same strength with less material. This averts a massive CO_2 emission in the production of structural materials. CNTs have the highest measured tensile strength of all materials and form strong composites, but until recently, they were produced only by high carbon footprint processes. CNTs are synthesized in this study from CO_2 (are carbon negative) by low-energy C2CNT (CO_2 to CNT) molten electrolysis. Four tonnes of CO_2 electrolyzed forms one tonne of CNTs. This avoids several hundred tonnes of CO_2 by replacing structural materials with CNT composites. For example, a 2-tonne cement block with 0.001 tonne of CNTs has the same strength as a 3-tonne block without CNTs. The 1-tonne cement avoided eliminates its CO_2 production emission. Specifically, a 0.048 wt% CNT-cement composite eliminates 840 tonne of CO_2/tonne CNT. CO_2 is eliminated from the anthropogenic carbon cycle at less than $1 per tonne. High carbon footprint materials such as aluminum trigger larger CO_2 composite elimination effects, and 1 tonne of CNT extraordinarily eliminates more than 4000 tonne CO_2/tonne CNTs.

1. Introduction

Cement and metals are structural materials pervasively used in bridges, roads, architectural structures, vehicles, and industrial and consumer appliances. However, their production is greenhouse gas–intensive. For example, cement production alone accounts for 4–7% of all anthropogenic CO_2 emissions. Society consumes more than 3×10^9 tonne of cement annually, and the cement industry releases 9 kg of CO_2 for each 10 kg of cement produced, that is, a carbon footprint (f_c) of 0.9 tonnes CO_2 per tonne cement. The majority of CO_2 emissions occurs during the decarbonation of limestone ($CaCO_3$) at approximately 900 °C to lime (CaO) in a reactor and the remainder (30–40%) from burning fossil fuels, such as coal, to heat the reactor [1–4]. Virgin aluminum production is one of the most greenhouse gas–intensive industrial processes emitting f_c (carbon footprint) of 11.9 tonnes of CO_2 for each tonne of aluminum produced [5,6]. Even greater, the magnesium industry releases f_c of 14 tonnes of CO_2 for each tonne magnesium produced [7]. Titanium production has a carbon footprint lower limit of $f_c = 8.1$ tonnes CO_2 per tonne Ti, which is higher when recycling is excluded [8]. The massive global annual production of stainless steel of 1.6 billion metric tonnes coupled with a high f_c of 6.15 tonnes of CO_2 emitted per tonne of virgin stainless steel produced, including 5.3 tonnes of CO_2 per tonne for energy to drive the production [8,9], provide a compelling incentive to reduce global greenhouse gas emission in this industry.

Several materials are stronger than cement, aluminum, steel, magnesium, or titanium. Carbon nanotubes (CNTs) have the highest tensile strength (93,900 MPa) of any material measured [10,11]. CNT composites have engaged a growing interest among the engineering and scientific community because of the observed substantial increases (higher than 10%) in beneficial mechanical properties such as tensile, compressive, and flexural strength with minimal addition (generally less than 0.1 wt%) of CNTs. Composites studied include CNT-aluminum, CNT-steel, CNT-magnesium, and CNT-titanium, and the most studied of CNT-composite structural material alternatives, CNT-cement. As summarized in Fig. 1, the number of published studies on CNT-cement (or mortar or concrete) composites has grown at an exponential rate in the past 15

* Corresponding author.
E-mail address: slicht@gwu.edu (S. Licht).

https://doi.org/10.1016/j.mtsust.2019.100023
2589-2347/

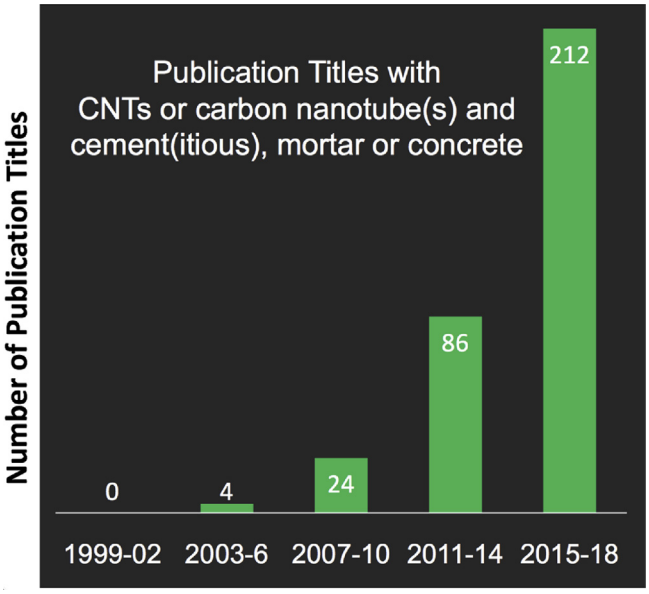

Fig. 1. The rapid growth of interest in CNT-cement composites as expressed by the number of published studies. A listing of these studies is available using the Web of Science and Google Scholar search engine in the 'title' category for CNT or carbon nanotube(s) and cement(itious), mortar or concrete. CNT, carbon nanotube.

years. Examples of these studies are included in the supplementary information appendix.

The conventional synthesis of carbon nanomaterials by chemical vapor deposition (CVD) has a massive CO_2-positive footprint, emitting as much as 600 tonnes CO_2 per tonne of carbon product [12]. Perhaps owing to this as well as the high conventional production costs of CNT synthesis, the carbon-negative CO_2 avoidance consequences of CNT composites had not been previously realized. In this study, the massive CO_2 avoidance of CNT composites is calculated for the first time. Here, a lower cost, carbon-negative process method to produce CNTs is delineated using CO_2 as the reactant.

2. Carbon nanotube – structural material composites

The tensile, compressive, and flexural strength increase of cement, mortar, and concrete with the addition of small amounts of CNTs has been widely reported [13–18]. Homogenous dispersion of the CNTs and interaction with the cement has been achieved with techniques including sonication, addition of surfactants, and stirring. Sonication dispersion processes do not add a significant power [19] or related CO_2 emissive component. The cost impact in the industrial production chain still needs to be determined. CNT aqueous dispersion and addition in the cement aqueous mix step is not a complex process, and stable aqueous CNT dispersion lifetimes of at least 4 years have been measured [20]. In a comparison of CNT and cement mixes with 0.5- to 30-μm CNTs ranging from 0.03 to 0.25 wt% in the composite, longer CNTs attained higher strength composites [15]. Similarly, pure CNTs with a length of ~200 μm, exhibited higher tensile strength than shorter length CNTs [11]. In the composite, an addition less than 0.05 wt% CNT to cement increases tensile (S, % strength increase), S = 45% is the typical of the reported large increases in cement strength with small additions of CNTs (as delineated in 300 + titles in the supplementary data).

CNT-metal composites have also been of interest. Processes to disperse CNTs in the preparation of a CNT-Al composite have been compared [21,22], and the addition of 0.1 wt% CNT to an aluminum composites increases aluminum tensile strength by 37% [23]. Homogeneous dispersion of CNTs in CNT-magnesium composites has been challenging. CNT agglomeration inhibits formation of effective magnesium composites decreasing the CNT-metal interaction. Nai et al. [24] have overcome this through nickel coating of the CNTs providing an effective CNT-Mg_2Ni interface, and their 0.3 wt% CNTs-magnesium composite exhibits an increased tensile strength of 39%. The higher melting point and processing temperatures of titanium or steel than aluminum and magnesium poses challenges to create a uniform dispersion of CNTs in the composite, and there have been fewer reports of CNT-Ti or CNT-steel composites than with other metals [25–29]. In a CNT-titanium composite, 102% tensile strength increase occurred with inclusion of 0.3 wt% CNT [25]. Patel et al. formed a 4 to 6 wt% CNT–stainless-steel composite using CVD to infiltrate CNTs directly into stainless-steel pellets. The resulting composite had a substantial increase in the elastic modulus, yield strength, and hardness by 47, 104, and over 93%, respectively [28]. Loayza et al. [29] incorporated 0.75 wt% CNTs, and as with the high-strength titanium composite also using a Ni-coated CNT, into 316 stainless steel via pulsed tungsten arc welding. The 0.75 wt% CNT-stainless steel composite exhibit 35% higher Vickers hardness (which can be correlated with yield strength). Cho et al. incorporated ~0.75 wt% (3 vol%) CNTs by ball milling into 304 stainless steel. The 0.75 wt% CNT-stainless steel composite exhibits 37% higher yield strength [30].

3. CNT production

3.1. Traditional methodologies for CNT syntheses

Perhaps owing to their previous perception as costly, the sustainability implications of structural material CNT composites had been disregarded. However, as the material with the highest measured tensile strength, CNTs can avoid carbon emissions from humanity's pervasive use of structural materials. CNT composites have not been previously synthesized with CNTs made from CO_2. CNTs have been synthesized by several methodologies including flame-assisted and plasma-assisted CVD techniques [31–36]. CNT demand is mainly limited by the complexity and cost of those synthetic processes, which requires 30- to 100-fold higher production energy than for aluminum [37,38]. Owing to the expense, energy intensity, and complexity of the synthesis, industrial CNTs currently are valued in the $100K ($85-$450K) per ton range and do not use CO_2 as a reactant [36–39]. For CVD processes, the cost, complexity, and impacts may eventually be significantly reduced by using a continuous rotary or fluidized bed reactor and by using alternative support and catalyst materials.

3.2. Experimental. A new CNT synthesis: C2CNT – CO_2 to CNT

We recently discovered a high-yield, high-purity, (low) electricity cost–constrained CNT synthesis, C2CNT (CO_2 to CNTs) [39–41]. C2CNT splits carbon dioxide by electrolysis in molten carbonates. The physical chemical environment of the conventional CVD CNT synthesis is different than that of the new C2CNT synthesis in many aspects. The latter is an electrochemical process, while the former is a chemical one. CVD generally utilizes organometallics as the reactant, while C2CNT consumes only CO_2 as the reactant. CVD generally occurs at a gas/solid interface, while C2CNT occurs at the liquid/solid interface. There are also significant subtle differences. C2CNT provides a higher density of reactive carbon (the molten carbonate electrolyte) near the growth interface. An electric field may, or may not, be applied to the substrate during CVD CNT growth, and there is always an intense electric field rapidly decreasing through the double layer adjacent to the cathode during

C2CNT growth. Isotopic ^{13}C tracking was used to follow CO_2's consumption as it is dissolved in molten carbonate and is split by electrolysis to form the building blocks of CNTs [40]. C2CNT transforms CO_2 to CNTs by molten electrolysis [39–51]. Transition metal–nucleated electrolysis in lithium carbonate (pure or with added oxides [39,42,50], added sodium, calcium, or barium carbonates [42,44], or added boron, sulfur, phosphorus or nitrogen dopants [41,42,49]) forms CNTs, oxygen, and dissolved lithium oxide:

$$Li_2CO_3 \rightarrow C_{CNT} + O_2 + Li_2O \quad (1)$$

CO_2 added to the electrolyte dissolves and chemically reacts with lithium oxide to renew and reform Li_2CO_3:

$$CO_2 + Li_2O \rightarrow Li_2CO_3 \quad (2)$$

Transition metals, such as Ni or Cr, nucleate CNT formation [39,41,45] and comprise less than 0.1% by mass of the product and can be variously added to the electrolyte or cathode or added by leaching from the anode. The net reaction of Eqs. (1) and (2) is splitting of CO_2 by electrolysis to CNTs and oxygen:

$$CO_2 \rightarrow C_{CNT} + O_2 \quad (3)$$

CO_2 dissolution in molten lithium carbonate is exothermic and rapid, which along with heat generated by the electrolysis provides thermal balance as shown in Supplementary Data Fig. 1.

At 750 °C, a carbon product can be formed in pure Li_2CO_3, mixed binary, and ternary lithiated and lithium-free molten carbonates [39–46,49,52]. Analogous to the case of the production costs of aluminum smelting by electrolysis of the oxide (bauxite) in a molten salt, the cost of CNTs by electrolysis of carbon dioxide in a molten salt (molten carbonates) is only the order of $1000 per tonne [42]. As with aluminum production that occurs at temperatures above 900 C, CNT production at temperatures above 700 °C forms a high-purity CNT product. Electrolysis temperatures lower than 700 °C or the inclusion of K_2CO_3 in the molten carbonate electrolyte tends to form a lower fraction of CNTs in the carbon product. Molten carbonate electrolytes mixed with hydroxide in the 480–650 °C domain form a solid carbon electrolysis product along with hydrogen or methane [56,57].

The focus of this study is theoretical calculations of greenhouse gas CO_2 reductions using CNT composite structural materials when formed with CNTs made from CO_2, rather than conventional high-CO_2-emissive production techniques such as CVD. In line with that theoretical focus, we also include experimental results of CNTs produced by molten carbon electrolytic splitting of CO_2. As shown in Fig. 2 using a PHENOM Pro-X SEM (top), or FEI Teneo LV SEM bottom), the electrolysis product from CO_2 (C2CNT) in 770 °C molten lithium carbonate is short thick (Fig. 2A), short thin (Fig. 2B), or long (Fig. 2C) CNTs as synthesized on simple (non-noble) metal cathodes such as a copper, stainless steel, or Monel cathode. In each case, the product forms on the 5-cm^2 cathode during constant current electrolysis, and after electrolysis, the cathode is extracted and the cooled black product peeled off the electrode and washed before microscopy as previously delineated [38]. We demonstrated tangled 5- to 8-μm-long CNTs grown on a copper cathode as nucleated with Ni powder added to the electrolyte to provide nucleation points for

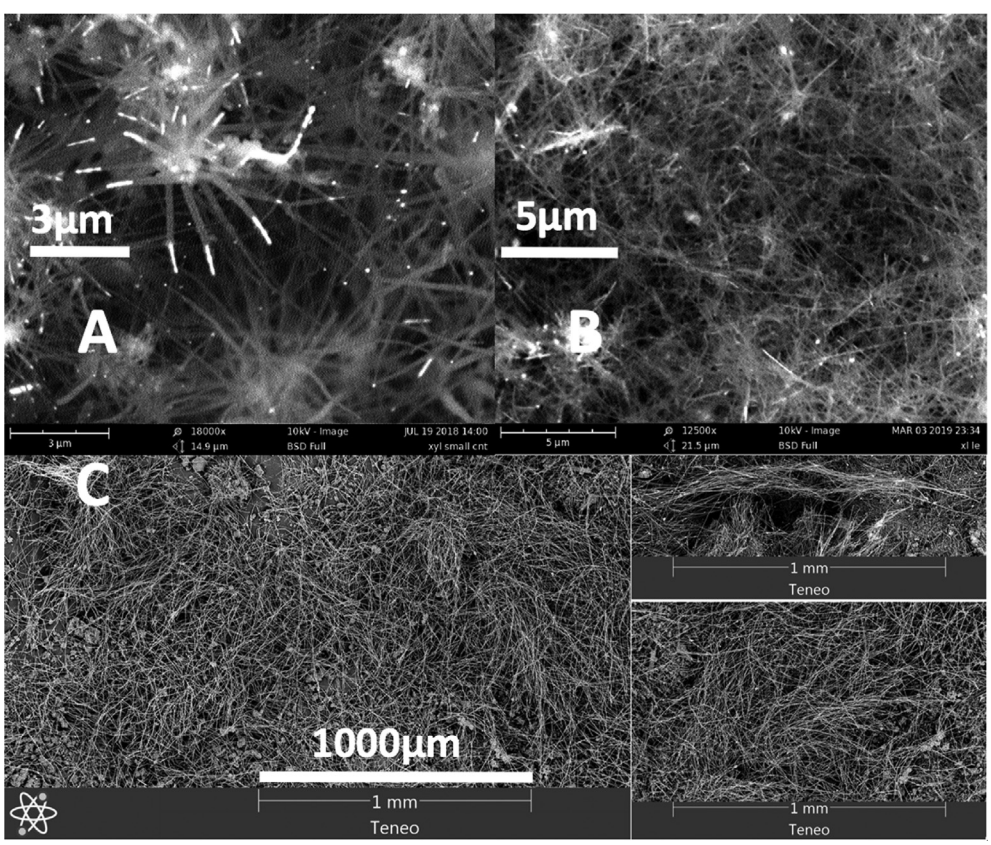

Fig. 2. (A) Short thick, (B) short thin, and (C) long C2CNT carbon nanotubes synthesized by electrolysis of carbon dioxide. In molten Li_2CO_3 at 770 °C, CNTs are synthesized (A) using copper cathode, (B) using a stainless-steel cathode, and (C) using a Monel cathode. CNT, carbon nanotube.

CNT growth [42]. Here, on a copper cathode, we synthesize straight 5- to 10-μm-long CNTs from nickel nucleation points as shown in Fig. 2A. The straight CNTs are formed when excess Ni powder is pasted directly on the copper cathode before electrolysis. As previously presented and as summarized in the bottom of Fig. 2B, when an extended charge, Monel cathode− and nickel- and chromium-induced nucleation electrolysis is instead applied, a high yield of very long CNTs, i.e., 200–2000 μm, is produced [41]. As summarized in Fig. 3, the control of electrolysis conditions produces controlled, uniform thickness, and either twisted, straight, or thicker straight CNTs. The short C2CNT CNTs described in Fig. 2A (a copper cathode in molten 770 °C Li_2CO_3) are produced by electrolysis for either 15, 30, or 90 min to yield thin- (~20 nm), medium- (~47 nm), or thick- (~116 nm) walled CNTs as evident by transmission electron microscopy (TEM), as shown in Fig. 3A, B and 3C, respectively, and exhibiting the distinctive graphene-layered characteristic 0.335-nm separation between concentric cylindrical walls. The lower section of Fig. 3 presents the CNT product after synthesis for 5 h using a brass cathode under various controlled conditions to yield bunched (Fig. 3D), straight (Fig. 3E), or thicker (Fig. 3F) CNTs.

Details of small- and large-scale C2CNT syntheses are referenced in the Supplementary Data. C2CNT is currently being scaled as shown in Fig. 4, up to 2–5 tonnes CO_2 removal daily as one of five Carbon XPrize finalists to transform the greenhouse gas carbon dioxide to the most valuable product at a natural gas power plant as detailed in [55]. The production at laboratory scale has a higher specific cost and environmental impact than that at industrial scale.

Homogeneous dispersion of CNTs is key to the formation of strong composites. For example, tangled CNTs agglomerate and are not readily miscible in aqueous mixtures. Modification of C2CNT electrolysis conditions provides precise control over the CNT product morphology. Untangled CNTs with a high aspect ratio (Fig. 5A) readily disperse in water with sonication and without the need of a surfactant (Fig. 5B), and the water-dispersed CNTs are mixed to form CNT-cement composites (Fig. 5C).

Alkali (lithium, sodium, and/or potassium) carbonate mixtures are less viscous than the pure molten carbonate salt [58–60]. We avoid anodic corrosion during C2CNT electrolysis by exclusion of potassium carbonate from the electrolyte [53]. Here, CNTs are formed by electrolysis in a low-viscosity binary lithium-sodium carbonate electrolyte, and we have additionally observed that the addition of metaborate salt to the electrolyte improves the aspect ratio. The product scanning electro microscopy image shown in Fig. 5A is that of 90% CNTs, and the electrolysis occurred at 97.5% coulombic efficiency (determined using Eq. (3) comparing the moles of carbon product to the integrated electrolysis current). As will be shown, small quantities of such CNTs added at a low concentration (less than 0.8%) form cement or metal composites having the same strength but decreased mass by at least 25%.

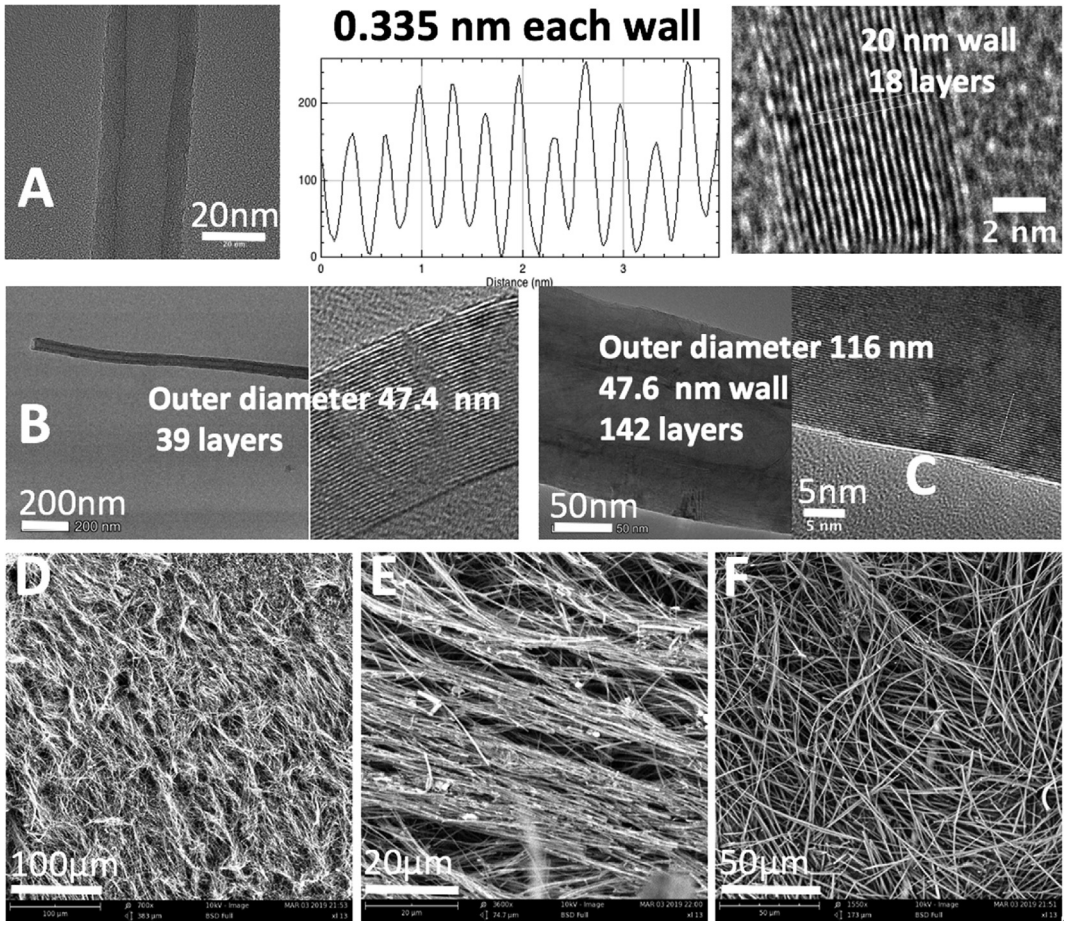

Fig. 3. Molten carbonate electrolysis conditions, such as electrolysis time, cathode material, or addition of oxide to the electrolyte, control the C2CNT CNT thickness and whether the CNTs are bunched or straight. (A–C) TEM images of short C2CNT carbon nanotubes synthesized as described in Fig. 2 – grown on a copper cathode in molten Li_2CO_3 at 770 °C for an electrolysis time of 15 min (A), 30 min (B), or 90 min (C). Synthesis for 5 h using a brass cathode under various controlled conditions yields bunched (D), straight (E), or thicker (F) CNTs, as shown by SEM. CNT, carbon nanotube; SEM, scanning electron microscopy; TEM, transmission electron microscopy.

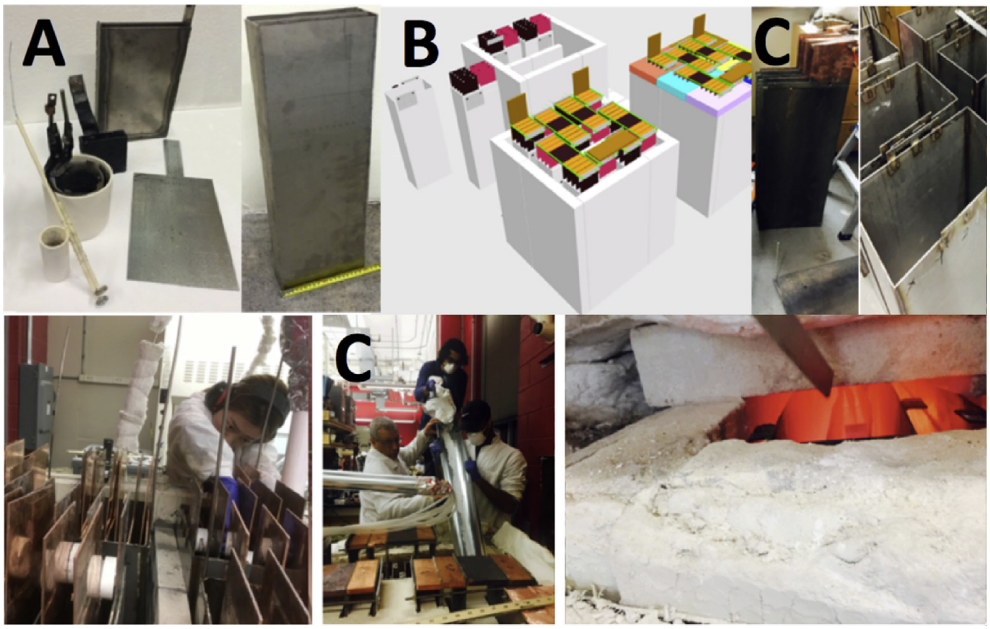

Fig. 4. C2CNT carbon dioxide modules are readily scalable and proportional to the electrode surface area. Modeling, building, and demonstration of the electrolyzer for the 0.2 tonne daily conversion of CO_2 to CNTs is shown [54]. (A) Increasingly scaled C2CNT electrolyzer cells and electrodes from 2015 to 2017. Diagrams (B) and photos (C) are of a 0.2-tonne daily CO_2 to CNT electrolyzer. CNT, carbon nanotube.

4. CO_2 avoidance of CNT composites

4.1. Massive CO_2 avoidance of CNT-cement composites

Conventional (non−CO_2-based) synthesized CNTs have a high carbon footprint and production cost. Likely, owing to these reasons, their carbon-negative, large CO_2 avoidance consequences had not been previously realized. CNTs are cost-effectively synthesized using CO_2 as the reactant and cast as composites, for example, as CNT-cement composite as shown in Fig. 5C, but how much CO_2 can be avoided by the CNTs? As illustrated in Fig. 6A, replacement of a large mass of cement with a small mass of CNTs forms a lower mass composite of equal strength (that is, higher strength per cross section multiplied by a smaller cross section) to the CNT-free cement, which avoids the large carbon dioxide emission of the replaced cement. The tensile, compressive, and flexural strength increase of cement with the addition of small amounts of CNTs has been widely reported [13−16]. In the more than 300 studies summarized in Fig. 1, as delineated by the titles collated in the supplementary material, the range of CNT additives is consistently small. This additive is generally less than 0.1 wt%, and the strength increase, whether tensile, compressive, and/or flexural, is large, generally in the range of 30−60%, without sand (cement), with sand and/or fly ash (mortar), or with sand and gravel aggregates (concrete). There are a variety of strength increase reports of more than 50% in CNT-cement composites [61−66]. Examples for CNT-concrete composites include increases of 45% compressive strength, 31% flexural strength, and 42% fracture energy [67]; a 37% increase in cracking load and a 25% increase in flexural strength with 0.05% CNT [15]; increases of 21% compressive, 35% tensile, and 14% flexural strengths with 0.03% CNT [68]; and up to 118% increase in toughness (resistance to brittle failure) [69]. Although reported strength trends vary, presumably owing to variations in CNT quality and dispersion methodologies, generally an increase in compressive strength is accompanied by increases in tensile and flexural strengths, for example, increases of 58%, 22%, and 38%, respectively, with 0.05−0.1 wt% added CNT-cement composites [70]. These comprehensive strength increases with CNT addition are of profound importance because of the wide variety of useful cement strength and antifracture properties and applications from unreinforced cements and mortars such as those used to fill voids in injection grouting for repair and in rig cement and cement blocks and to bind bricks and for unreinforced and reinforced (for example rebar reinforced) concrete usage such as in countertops, building structures, and cement pavement for roadways.

To introduce the fundamental new calculation of carbon dioxide avoidance through the composites, we assume here (i) a strength increase of 45%, (ii) a generic composite estimate of 0.048 wt% CNT addition to cement, and (iii) a conventional, direct cement usage (such as a cement block). An addition of 0.048 wt% CNT to cement which increases tensile strength, S, by 45% is typical of the reported large increases in cement strength with the small addition of CNTs. It is interesting to note that CNT increases the composite tensile, compressive, and flexural strength with minimal CNT addition acting as a 'nanorebar' tending to make CNT-cement less brittle. For strength applications, concrete is generally used as it has load-bearing capacity, whereas cement is brittle and less useful. Reported CNT-concrete strength increases are comparable with those of CNT-cement strength increases (Supplementary Data compiled study titles), and the usage here of the term 'CNT-cement composite' generically refers to both CNT-cement and CNT-concrete composites. Thinner cement composite with added CNTs will have the same strength as thicker cement. In a simple-usage case, such as a thinner block to bear the same load but with a 45% stronger CNT-composite, a 1/1.45 (or 69%) as thick, CNT-cement composite has the same strength as the cement without CNT, that is, a composite of 1 tonne CNT (0.048 wt%) in 2082 tonnes of cement has the same strength as 3021 tonnes of cement. The elimination of structural material mass in the composite is derived from the respective W (composite) and N (non-composite) mass in tonnes,

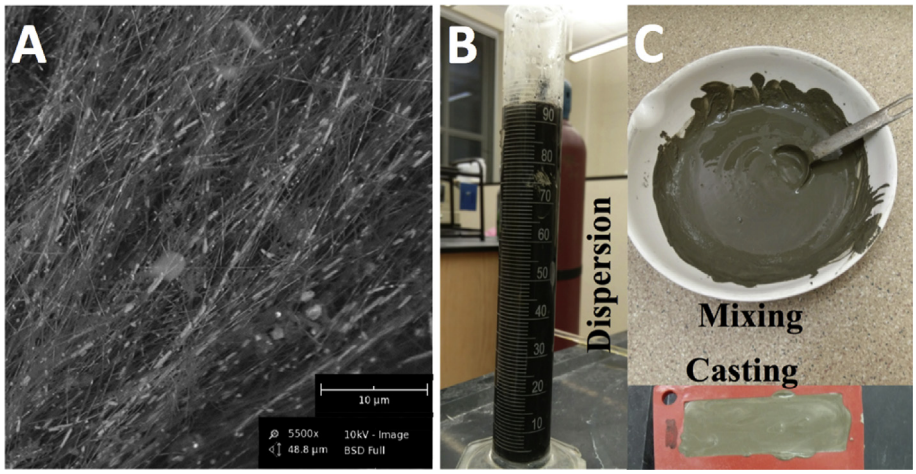

Fig. 5. (A) Untangled CNTs are synthesized at 740 °C in a mixed molten carbonate containing (by wt%) 73% Li_2CO_3, 17% Na_2CO_3, and 10% $LiBO_2$ by electrolysis using a brass cathode and an Inconel cathode. (B) During sonication, CNTs readily disperse in water without the addition of surfactants. Without sonication, CNTs agglomerate and the homogenous black liquid is not formed. (C) Upon mixing the aqueous dispersed CNTs with Portland cement, the mix is readily cast as CNT-cement composites. CNT, carbon nanotube.

from C, the CNT wt% concentration, and from S, the strength increase. The composite mass, W, that contains 1 ton CNT is in tonnes

$$W = 100\%/C \tag{4}$$

The non-composite weight, N, is determined from the strength and relative weight of the composite mass in tonnes:

$$N = W \times (100\% + S) / 100\% \tag{5}$$

As illustrated in Fig. 6, the tonnes weight decrease in the composite compared with the non-composite = N − W, and upon substitution of Eqs. (4) and (5), the weight decrease in the composite is in tonnes

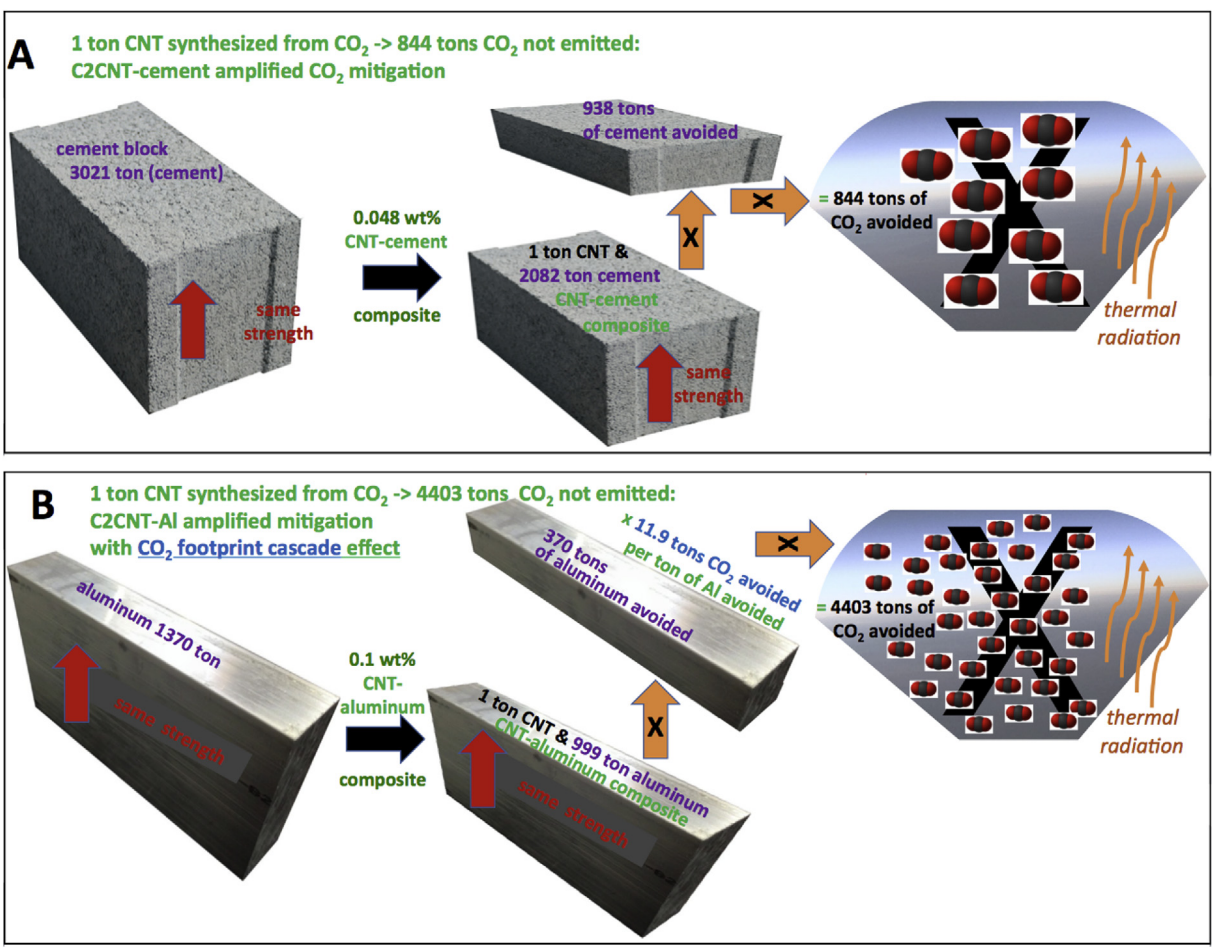

Fig. 6. Massive carbon dioxide avoidance by the addition of carbon nanotubes synthesized from CO_2 to CNT-composites. (A) Carbon mitigation with CNT-cement. (B) Carbon mitigation with CNT-Al. The latter (B) includes a cascade effect due to virgin Al's large carbon footprint, triggering larger CNT-composite induced CO_2 emission elimination. In the figure "ton" refers to metric tonne and CNT, carbon nanotube.

$$=N-W\ =W(100\%+S)/100\%-W\ =W\times(S/100\%)=S/C \quad (6)$$

Hence, the CNT-cement composite eliminates the need for 938 tonnes of cement (=S/C). One tonne of CNTs replaces 938 tonnes of cement to achieve the same strength. These values are summarized in Table 1 and are illustrated in the left and middle portions of Fig. 6A.

The cement industry releases 0.9 tonne of CO_2 for each tonne of cement produced [1–4]. Using the CNT-cement composite, the tonnes of CO_2 avoided per tonne of CNT are calculated in Table 1 from the product of the tonnes of cement replaced (per tonne of CNT used in the composite) and 0.9 tonnes of CO_2 emitted per tonne of cement produced. This avoidance of 844 tonnes of CO_2 per tonne of CNT is illustrated in the right side of Fig. 6A. Note that one dimension of strength increase is exemplified in this study. However, if the composite's increased tensile strength was utilized in multiple dimensions, then the formed cement is thinner in several dimensions and even greater mass reductions can be achieved with the stronger CNT composite.

4.2. CNT-amplified CO_2 avoidance of high carbon footprint metals

Compared with cements, to date, there are fewer studies on the strengthening effect of CNTs on metals although they too present a large strength increase in the metal with a small CNT additive (composite). The massive tonnage (844 tonnes) of CO_2 avoided per tonne of CNT in a cement composite can be surpassed, when the virgin material displaced by CNTs has a carbon footprint greater than 1. In this case, the composite material leads to a cascade-multiplicative effect in which the elimination of one mass unit further leads to the elimination of many mass units. This is the case for the CNT-Al composite. As with CNT-cement, a key to effective, strong CNT-Al composites is the homogeneous dispersion of the CNTs within the composite [21,22]. Inductive heating and melting of aluminum provides an effective media to homogenously disperse CNTs as a CNT-Al composite. As with the cement composite, the addition of a small fraction of CNTs to an aluminum melt does not add a significant additional CO_2 emissive component to the aluminum preparation. The addition of 0.1 wt% CNT increases aluminum tensile strength by 37% [23]. Hence, for a simple (one-dimensional applied force) usage case as summarized in Table 1, such as a thinner CNT-Al composite foil to bear the same load, 1 tonne of CNT replaces S/C = 370 tonne of aluminum as illustrated in the middle portion of Fig. 6B.

Fig. 6A and B compare the carbon avoided through the use of a CNT-cement and a CNT-aluminum composite. As illustrated in Fig. 6B, the use of a CNT-Al composite avoids an extraordinarily high value of 4403 tonnes of CO_2 upon addition of 1 tonne of CNT because of the cascade effect of a high carbon footprint in the production of aluminum. By relative mass, aluminum production is one of the most greenhouse gas–intensive industrial processes emitting $f_c = 11.9$ tonnes of CO_2 for each tonne of aluminum produced [5,6]. This value and the CO_2 avoidance of 4403 tonnes of CO_2 per tonne CNT are summarized in the right side of Fig. 5B and Table 1.

CO_2 elimination can be magnified through other large carbon footprint structural materials. In CNT-Mg composites, an uneven dispersion of CNTs decreases effectiveness of the CNT-metal interaction [22,71,72]. Dispersion has succeeded through effective Mg_2Ni interface between Mg and the CNT by first nickel coating of the CNTs. CNT (0.3 wt%) as a CNT-magnesium composite exhibits an increased tensile strength of 39% [24]. Magnesium production releases $f_c = 14$ tonnes of CO_2 per tonne of magnesium [7]. From this high footprint and the stronger composite made with low CNT additions, 1820 tonnes of CO_2 are avoided per tonne of CNTs in the CNT-Mg composite. These values are summarized in Table 1.

As previously noted, the higher melting point of titanium and steel than that of aluminum and magnesium structural metals poses challenges to create a uniform dispersion of CNTs in the CNT composite, and there have been fewer reports of these CNT composites than with other metals [25–29]. A CNT-Ti composite with inclusion of 0.3 wt% CNT exhibits a 102% tensile strength increase [27]. As summarized in Table 1, this composite proportionally replaces 339 tonnes of titanium by 1 tonne of CNT. With a carbon footprint of titanium production of $f_c = 8.1$ tonnes CO_2 per tonne Ti [8], 2750 tonnes of CO_2 are avoided per tonne of CNT in the CNT-Ti. Starting with widely used stainless steel (SS 304), Cho et al. [30] incorporated by 3 vol% CNTs ball milling. The ~0.75 wt% CNT-stainless steel composite exhibits 37% higher yield strength. Coupled with the high carbon footprint, $f_c = 6.15$ tonnes of CO_2 emitted per tonne of stainless steel [6,9], this avoids 302 tonnes of CO_2 per tonne CNT in the CNT-stainless steel composite as summarized in the final row of Table 1.

5. C2CNT CNT composite energy balance and energy consumption

5.1. C2CNT energy recovery through the O_2 product

C2CNT splits CO_2 by electrolysis forming CNTs. The second product of the C2CNT process (in addition to CNT) is hot oxygen. As delineated in the Supplementary Data, this product is useful in a range of industrial processes. Compared with air, oxygen improves the efficiency of ozone generation and is an essential feedstock in

Table 1
CO_2 avoidance of CNT-X (X = cement, Al, Mg, Ti, or stainless steel) composites.

X	wt% CNT	Property	Increase in property	Tonnes X removed per tonne CNT to achieve equal strength	Tonnes CO_2 emitted per tonne X produced	Tonnes CO_2 avoided per tonne CNT	kWh consumed per tonne CO_2 avoided
Cement	0.048%	Tensile strength	45%	938	0.9	**840**	**2.45**
Aluminum	0.10%	Tensile strength	37%	370	11.9	**4400**	**0.47**
Magnesium	0.30%	Tensile strength	39%	130	14	**1820**	**1.14**
Titanium	0.3%	*Yield strength*	102%	339	8.1	**2750**	**0.75**
Stainless steel	0.75%	Tensile strength	37%	49	6.15	**302**	**6.85**

CNT, carbon nanotube.
The final column of the table normalizes the net energy consumed by CNT production in the Energy consumption section 5.2 by the CNT's CO_2 avoidance.

the manufacture of a variety of industrial chemicals. Using oxygen in lieu of air consumes proportionally less fuel or generates a higher combustion temperature. The fuel savings by retrofitting air/fuel systems with oxy/fuel is 30–60% for the steel, copper, aluminum, lead, and glass industries and 50% for waste incineration and sulfuric acid recovery.

Oxygen is conventionally produced principally by cryogenic cooling. Pure oxygen separation from air requires a thermodynamic energy of 53.1 kWh/tonne and a practical energy of 196 kWh/tonne oxygen. Heating oxygen to 770 °C requires an additional enthalpy of 0.22 MW/tonne O_2. As delineated in the supplementary data, the C2CNT hot oxygen product has an energy value:

$$\text{Conventional energy to produce hot } O_2\,(770^{\circ}C) = 0.4\text{MWh / tonne } O_2 \tag{7}$$

5.2. Energy consumption CO_2 avoided for CNT composites

As delineated in the SI, the net energy required by the C2CNT transformation of CO_2 to CNTs, including the energy recovered of one O_2 per CO_2 electrolyzed using the hot oxygen product in Eq. (7), is

$$E_{C2CNT}, \text{net energy consumed} = 2.0\text{MWh per tonne } CO_2 \text{ reacted to CNT } (1.6\text{MWh at } 0.8V) \tag{8}$$

The C2CNT net energy used in the CNT synthesis, Eq. (8), will decrease further with heat recovery from the hot CNT product, with excess heat from the dissolution reaction of CO_2 in carbonate, and from additives (such as oxides or borates), which decrease the electrolysis potential to ~0.8 V.

The massive (tonnes) of CO_2 avoided per tonne of CNTs in cement-, aluminum-, magnesium-, titanium-, or stainless steel–CNT composites is summarized in Table 1. The higher strength per unit weight of the CNT-cement composite than that of cement avoids 840 tonnes of CO_2 per tonne of CNTs in the composite. Al-CNT composite avoidance is even larger at 4400 tonnes CO_2 per tonne of CNT because of the higher CO_2 emission per tonne of Al produced. The final column of Table 1 normalizes the net energy consumed by C2CNT transformation of CO_2 to CNTs and O_2 in Eq. (8) by this CO_2 avoidance. The less than 7 kWh per tonne energy to eliminate a portion of the greenhouse CO_2 from the anthropogenic carbon cycle is lower than the current discussed tax credits for carbon capture which generally range above $30 tonne per CO_2. Based on kWh costs of electricity ranging from a low value of $0.029 per kWh for Texas wind [7] up to a conventional cost of $0.10 kWh, the final column costs range from $0.01 per tonne as a minimum cost for carbon avoidance with the CNT-Al composites to a maximum value of $0.69 per tonne CO_2 for carbon avoidance with the CNT-stainless steel.

Larger C2CNT syntheses have been reported [73] and recently conditions of the CO_2 molten carbon electrolysis modified to produce a variety of other carbon nanomaterials (CNMs) such as carbon nanoplatelets, graphene, graphene scaffolds and carbon nano-onions [74], each with a unique morphology and useful properties. As with CNTs, each is also readily dispersed in water by sonication to produce an aqueous disperion which can be mixed to produce a CNM-composite, such as CNM-cement, or mixed at higher temperature to produce CNM-metal composites such as CNM-aluminum.

6. Conclusions

CNTs are switched around from a massive (CVD production induced) carbon footprint material to a massive CO_2 avoidance material through their production by CO_2 electrolysis C2CNT and applications as lighter weight, strong CNT composite structure material. CNTs have the highest measured tensile strength of all materials and form strong composites. CVD production of CNTs emits hundreds of tonnes of CO_2 per tonne CNT, whereas C2CNT-produced CNTs avoid hundreds of tonnes of CO_2 per tonne CNT as CNT composites. The large carbon avoidance and low energy cost provide a compelling greenhouse gas mitigation incentive to drive conventional structural materials replacement by the CNT composites. The global CO_2 emissions of cement, aluminum, magnesium, titanium, and steel production are more than 2 gigatonnes of CO_2 per year (1.5 Gt CO_2 from cement alone). For example, a 0.048 wt% CNT-cement composite eliminates 840 tonnes of CO_2/tonne CNT. CO_2 is eliminated from the anthropogenic carbon cycle at less than $1 per tonne. Replacement of these with CNT-aluminum, CNT-magnesium, CNT-titanium, or CNT-stainless steel composites will significantly decrease the global annual anthropogenic emission of the greenhouse gas carbon dioxide to help mitigate climate change. This averts a massive CO_2 emission in that production. A life cycle assessment where long-term effects pertinent to individual applications are considered will be coupled in the future with experimental optimization of CO_2 transformed to CNTs physical properties (composite fracture resistance; tensile, flexural, and compressive strength; and composite lifetime tailored to the application).

Acknowledgments

The authors are grateful to the Carbon XPrize award for funding a portion of this research.

Author contributions

X.L., X.W., and A.S. conducted the described syntheses under the direction of S.L. D.C. interpreted mechanical strength with S.L. S.L. wrote the manuscript and determined the CNT composite strength, carbon avoidance, and energy calculations with input from G.L.

Conflict of interest

The authors declare no competing interests except that the authors are team C2CNT competing for the Carbon XPrize (CarbonXPrize.org) and are grateful to the Carbon XPrize award for funding a portion of this research.

Appendix A. Supplementary data

Supplementary data to this article can be found online at https://doi.org/10.1016/j.mtsust.2019.100023.

References

[1] R.M. Andrew, Earth Syst. Sci. Data 10 (2018) 195–217.
[2] Cement Technology Roadmap, International Energy Agency, available at: https://www.iea.org/newsroom/news/2018/april/cement-technology-roadmap-plots-path-to-cutting-co2-emissions-24-by-2050.html.
[3] S. Licht, H. Wu, C. Hettige, B. Wang, J. Asercion, J. Lau, J. Stuart, Chem. Commun. 48 (2012) 6019–6021.
[4] J. Allwood, J. Cullen, R. Milford, Environ. Sci. Technol. 44 (2010) 1888.
[5] Carbon Footprint Guidance Document, International Aluminum Association; http://www.world-aluminium.org/media/filer_public/2013/01/15/fl0000169.pdf.
[6] Emission factors in kg CO2-equivalents per unit. http://www.winnipeg.ca/finance/findata/matmgt/documents/2012/682-2012/682-2012_Appendix_H-WSTP_South_End_Plant_Process_Selection_Report/Appendix%207.pdf.
[7] S. Ehrenberger, H. Friedrich, Light Met. Age (2014) 50–53. February.
[8] P. Nuss, M. Eckelman, PLoS One 9 (2014), e101298, 1-12.
[9] J. Johnson, B. Reck, T. Wang, T. Graedel, Energy Pol. (2007).
[10] M.-F. Yu, O. Lourie, M. Dyer, K. Moloni, T. Kelly, R. Ruoff, Science 287 (2000) 637–640.
[11] C.-C. Chang, H.-K. Hsu, M. Aykol, W. Hung, C. Chen, S. Cronin, ACS Nano 4 (2010) 5095–5100.
[12] V. Khanna, B.R. Bakshi, L.J. Lee, J. Ind. Ecol. 12 (2008) 394–410.
[13] A. Hawreen, J.A. Bogas, A.P.S. Dias, Constr. Build. Mater. 168 (2018) 458–470.
[14] V.V. Rocha, P. Ludvig, Architect. Civil Eng. Env 2 (2018) 73–77.
[15] B. Mahesh, K. Rajeev, IJARIIE 4 (2018) 2526–2529.
[16] G.I. Yakovlev, G. Skripkiunas, I.S. Polianskick, O. Lahayne, J. Enerhardsteiner, L.A. Urkhanova, I.A. Pudov, S.V. Sychugov, E.A. Karpova, S.A. Sen'kov, Procedia. Eng. 172 (2017) 1261–1269.
[17] F. Ubertini, S. Laflamme, A. D'Alessandro, in: K.J. Loh, S. Nagarajaiah (Eds.), Innovative Developments of Advanced Multifunctional Nanocomposites in Civil and Structural Engineering, Woodhead Publishing, 2016, pp. 97–120.
[18] M.S. Konsta-Gdoutos, Z.S. Metexa, S.P. Shah, Cement Concr. Res. 40 (7) (2010) 1052e1059.
[19] T. Jarolim, M. Labaj, R. Hela, K. Michnova, Adv. Mat. Sci. Eng. 2016 (2016) 1–6.
[20] S. Parveen, S. Rana, R. Fangueiro, M.C. Paiva, Powder Technol. 307 (2017) 1–9.
[21] A. Umma Maleque, A. Iskandar, Y. Mohammed, Australian J. Bas. Appl. Sci. 6 (2012) 69–75.
[22] N. Silvestre, Int. J. Compos. Mater. 3 (2013) 38–44.
[23] M. Mansoor, M. Shahid, J. Appl. Res. Technol. 14 (2016) 215–224.
[24] M. Nai, J. Wei, M. Gupta, Mater. Des. 60 (2014) 490–495.
[25] S. Li, B. Sun, H. Imai, T. Mimoto, K. Kondoh, Compos. Appl. Sci. Manuf. 48 (2013) 57–66.
[26] K.S. Munir, P. Kingshott, C. Wen, Carbon critical reviews in solid state & mat, Sciences 40 (2014) 38–55.
[27] F. Lia, P. Hao, J. Yia, Z. Chen, K.G. Prashanth, T. Maity, J. Eckert, Mater. Sci. Eng. A 722 (2018) 122–128.
[28] R.B. Patel, J. Liu, J. Scicolone, J. Mater. Sci. 48 (2013) 1387–1395.
[29] C. Loayza, P. Assunc, D. Cardoso, D. Borges, A. Filho, M. Reis, E. Braga, J. Compos. Mater. 52 (2018) 1899–1906.
[30] H. Cho, S. Lim, H.-H. Jin, J. Kwon, S.-J. Hong, C. Shin, J. Compos. Mater. (2018) 2755–2766.
[31] S. Iijima, Nature 354 (1991) 56–58.
[32] (a) T.W. Ebbesen, P.M. Ajayan, Nature 358 (1992) 220–222.(b) W.K. Hsu, J.P. Hare, H.W. Terrones, D. Kroto, R.M. Walton, Nature 377 (1995) 687.
[33] D. Janas, K.K. Koziol, Nanoscale 8 (2016) 19475.
[34] A. Magrez, S. Arnaud, J. Won, R. Smajda, et al., Materials 2 (2010) 4878–4890.
[35] X.L. Jia, F. Wei, Top. Curr. Chem. 375 (2017), https://doi.org/10.1007/s41061-017-0102-2.
[36] Cheaptubes.com. Cheaptubes: industrial grade carbon nanotubes, 2017. Available from: https://www.cheaptubes.com/product-category/industrial-carbon-nanotubes-products/.
[37] Pluscomposites, Composites: materials of the Future: - Part 4: carbon fibre reinforced composites, 2015 pluscomposites.eu/publications, at: http://www.pluscomposites.eu/sites/default/files/Technical%20series%20-%20Part%204%20-%20Carbon%20fibre%20reinforced%20composites_0.pdf.
[38] H.C. Kim, V. Fthenakis, Industr. Ecology 17 (2012) 528–541.
[39] J. Ren, F.-F. Li, J. Lau, L. Gonzalez-Urbina, S. Licht, Nano Lett. 15 (2015) 6142–6148.
[40] J. Ren, S. Licht, Sci. Rep. – Nature.com 6 (2016) 27760 1–2776010.
[41] M. Johnson, J. Ren, M. Lefler, G. Licht, J. Vicini, X. Liu, S. Licht, Mater. Today Energy 5 (2017) 230–236.
[42] M. Johnson, J. Ren, M. Lefler, G. Licht, J. Vicini, S. Licht, Data in Brief 14 (2017) 592–606.
[43] S. Licht, A. Douglas, J. Ren, R. Carter, M. Lefler, C. Pint, ACS Cent. Sci. 2 (2015) 162–168.
[44] J. Ren, J. Lau, M. Lefler, S. Licht, J. Phys. Chem. C 119 (2015) 23342–23349.
[45] G. Dey, J. Ren, T. El-Ghazawi, S. Licht, RSC Adv. 6 (2016) 27191–27196.
[46] H. Wu, Z. Li, D. Ji, Y. Liu, L. Li, D. Yuan, Z. Zhang, J. Ren, M. Lefler, B. Wang, S. Licht, Carbon 106 (2016) 208–217.
[47] J. Lau, G. Dey, S. Licht, Energy Convers. Manag. 122 (2016) 400–410.
[48] S. Licht, et al., J. CO_2 Utilization 18 (2017) 378–389.
[49] S. Licht, et al., J. CO_2 Utilization 18 (2017) 335–344.
[50] S. Licht, et al., J. CO_2 Utilization 12 (2013) 58–63.
[51] S. Licht, B. Wang, S. Ghosh, H. Ayub, D. Jiang, J. Ginley, J. Phys. Chem. Lett. 1 (2010) 2363–2368.
[52] F.-F. Li, J. Lau S. Licht, Adv. Sci. 5 (2015) 1–7, 1500260.
[53] S. Licht, Stabilization of STEP Electrolyses in Lithium-free Molten Carbonates, 2012 arXiv:1209.3512v1.
[54] S. Licht, Carbon Dioxide to Carbon Nanotube Scale-Up, 2017 arXiv: 1710.07246v1.
[55] https://carbon.xprize.org/prizes/carbon.
[56] F.-F. Li, S. Liu, B. Cui, J. Lau, J. Stuart, B. Wang, S. Licht, Adv. Energy Mat. 5 (2015) 1401491 1–7.
[57] H. Wu, D. Ji, L. Li, D. Yuan, Y. Zhu, B. Wang, Z. Zhang, S. Licht, Adv. Mat. Tech. 5 (2016) 1600092 1–160009210.
[58] S.W. Kim, K. Uematsu, K. Toda, M. Sato, J. Ceramic Soc. Jap. 123 (2015) 355–358.
[59] S. Lee, M. Kim, M. Hwang, K. Kim, C. Jeon, J. Song, Exp. Therm. Fluid Sci. 49 (2013) 94–104.
[60] T. Kojima, Y. Miyazaki, K. Nomura, K. Tanimoto, J. Electrochem. Soc. 155 (2008) F150–F156.
[61] J.L.G. Lim, S.N. Rman, R. Hamid, M.F.M. Zain, F.C. Lai, Jurnal Tecknologi 80 (2018), 371-282.
[62] L.J. da Silva, T.H. Panzera, L.M.G. Vierira, J.G. Duduch, C.R. Brown, J.C. Campos Rubio, J. Eng. Tribology 231 (2017) 1397–1407.
[63] X. Cui, B. Han, Q. Xeng, X. Yun, S. Dong, L. Zhang, J. Ou, Composites Part A 103 (2017) 131–147.
[64] M.O. Mohensen, N. Al-Nuaimi, R.K. Abu Al-Rub, A. Senouci, K.A. Bani-Hani, Constr. Build. Mater. 126 (2016) 586–598.
[65] M.S. Konstas-Gdoutos, P.A. Danoglidis, M.G. Falara, M.E. Maglogianni, E.E. ≥Gdoutos, ICTAEM 2018 (2018) 1–4.
[66] L. Restuccia, A. Lopez, G.A. Fero, D. Liberatore, J.M. Tulliani, Fatigue Fract. Eng. Mater. Struct. 41 (2018) 119–128.
[67] Y. Ruan, B. Han, X. Yu, W. Zhang, D. Wang, Composites Part A 112 (2018) 19–25.
[68] H. Elkady, A. Hassan, Sci. Rep. 8 (2018) 11243 1–1124311.
[69] W.L. Baloc, R.A. Khushnood, S.A. Memon, W. Ahmed, S. Ahmad, Fire Technol. 54 (2018) 1331–1367.
[70] H. Ahmed, J.A. Bogas, M. Guesdes, J. Mater. Civ. Eng. 30 (2018) 04018257 1–0401825714.
[71] C. Goh, J. Wei, I. Lee M. Gupta, Nanotechnology 17 (2005) 7–12.
[72] Q. Li, A. Vierecki, C. Tottmair, R. Singer, Compos. Sci. Technol. 69 (2009) 1193–1199. [73] X. Wang, X. Liu, G. Licht, B. Wang, S. Licht, *J. CO2 Utilization 34* (2019) 303-312. [74] X. Liu, J. Ren, G. Licht, X. Wang, S. Licht, *Adv. Sust. Sys.* (2019) 1900056 1-10..
[73] X. Wang, X. Liu, G. Licht, B. Wang, S. Licht, J. CO_2 Utilization 34 (2019) 303–312.
[74] X. Liu, J. Ren, G. Licht, X. Wang, S. Licht, Adv. Sust. Sys (2019) 1–10, 1900056.